1222+216: A WIDE-ANGLE-TAILED QUASAR?

D. J. SAIKIA

National Centre for Radio Astrophysics, Tata Institute of Fundamental Research, Poona University Campus, Post Bag No. 3,
Pune 411 007, India
Electronic mail: djs@gmrt.ernet.in

PAUL J. WIITA

Department of Physics & Astronomy, Georgia State University, Atlanta, Georgia 30303-3083 and National Centre for Radio Astrophysics, Pune, India Electronic mail: wiita@chara.gsu.edu

T. W. B. MUXLOW

Nuffield Radio Astronomy Laboratories, University of Manchester, Jodrell Bank, Macclesfield, Cheshire SK11 9DL, England Electronic mail: jbvad::tbm

Received 1992 September 21; revised 1993 January 22

ABSTRACT

We present Very Large Array and MERLIN images of the quasar 1222+216, whose radio structure is reminiscent of a wide-angle-tailed source. While such radio structures are common among radio galaxies of moderate power, they are rare among the luminous quasars. This quasar, with a redshift of 0.435 and a largest angular size of 19.6 arcsec, which corresponds to a linear size of ~ 131 kpc, occurs in a region of high galaxy density. This suggests that its structure could well be due to interaction of the radio emitting plasma with the external cluster environment. We examine the possibility that a rather abrupt bend is probably due to interaction of the jet with an external galaxy or cloud while larger scale features can be explained by the relative motion of the parent galaxy through the intracluster medium. We also discuss other possible scenarios and attempt to determine whether cluster membership or projection effects is the dominant factor responsible for the observed distortion of quasars.

I. INTRODUCTION

The majority of quasars selected from low-frequency radio surveys are reasonably collinear and have edgebrightened outer lobes. A significant fraction, however, exhibit large deviations from a collinear structure exhibiting a wide variety of shapes. They include the ones with misaligned axes, referred to as the "dog-leg" or "boomerangshaped" ones (Hintzen et al. 1983 and Hintzen 1984, hereafter referred to as HUO and H84, respectively; Stocke et al. 1985), the complex sources (e.g., Fanti et al. 1986; Pearson & Readhead 1988; Wilkinson et al. 1991), and the L- or C-shaped ones (e.g., Saikia et al. 1987) which look like the lower-luminosity wide-angle-tailed (WAT) radio galaxies (O'Donoghue, et al. 1990). However, all highly noncollinear quasars are often collectively referred to as WAT quasars (e.g., HUO; H84). Also, unlike their lowluminosity counterparts, the WAT quasars belong to class II of the Fanaroff-Riley classification scheme and usually have prominent hot-spots at their outer edges. The distorted structures seen in these quasars could be produced by deflection of the radio jets by strong density gradients, dense clouds or galaxies, or else by ram pressure due to the relative motion of the galaxy and the intracluster medium (Riley & Pooley 1978; Begelman et al. 1979; Harris et al. 1983; Liu & Pooley 1990). The intrinsic distortions could appear amplified if the source is inclined at a small angle to the line of sight.

The discovery of clusters of galaxies associated with quasars enables one to use the radio properties as a probe of the physical conditions and evolution of the cluster or group (e.g., H84; Yee & Green 1984, 1987; Smith & Heckman 1990; Ellingson et al. 1991). From observations of a sample of quasars, largely made by HUO, H84 attempted to compile a sample of WAT quasars and examine whether they occur in richer galaxy environments than the undistorted sources. In this paper, we study in some detail the most distorted WAT quasar considered by H84, namely 1222+216 (4C 21.35) which is at a redshift of 0.435. This source is embedded within a cluster which is clearly visible on a deep red CCD image of the field taken by H84. The quasar is over 2 mag brighter than any other object in the finding chart. We first present the results of the observations, discuss possible interpretations and then attempt to determine the dominant process responsible for the observed distortion of quasars. Although not as distorted as 1222+216, the quasar 3C 275.1 shows many similar properties, and has been observed in both the radio (Riley & Pooley 1978; Stocke et al. 1985; Liu & Pooley 1990) and optical wavebands (Hintzen et al. 1981; H84; Hintzen & Stocke 1986; Hintzen & Romanishin 1986), providing substantial evidence that interaction with a companion galaxy can explain the distorted structure.

The arcsec-scale structure of the quasar 1222+216 has been imaged earlier by Miley & Hartsuijker (1978), Neff (1982), and HUO, but all these observations did not have

1658 Astron. J. 105 (5), May 1993

0004-6256/93/051658-08\$00.90

© 1993 Am. Astron. Soc. 1658

TABLE 1. Observational parameters and observed properties of 1222+216.

Source	Observational parameters							Observed properties										
	Obs. Obs.					σ_t σ_p		Comp.	Radio position (B1950) Flux density Polarization									ization
	$_{ m date}$	λ	maj.	min.	PA		·			R. A	A .		Dec.		peak	total	%	PA
		cm	"	"	0	mJy/b	mJy/b		h	m	s	٥	,	"	mJy/b	mJy		0
(1)	(2)	(3)		(4)		(5)	(6)	(7)		(8)		(9)		(10)	(11)	(12)	(13)
1222+216	83Nov25	V20	1.33	1.29	24	0.43	0.14	S(A)	12	22	22.94	21	39	16.7	14	40	31	68
								S(B)			23.30		-	14.3	20	148	13	94
								C			23.41			22.7	704		3	82
								E			24.17			25.4	131	281	9.5	155
								Total							704	1875		
	83Nov25	V6	0.42	0.40	179	0.36	0.33	\mathbf{C}^g	12	22	23.41	21	39	22.8	655	676	2.6	88
								J1			23.44			23.7	40	63	15.6	139
								J2			23.49			24.1	31	64	3.3	136
								J3			23.58			23.3	4	16	\leq 24	
								E			24.19			25.7	11	106	27.2	37
								Total							650	934		
	83Feb 22	MV18	0.40	0.40		0.18		S(A)							~3	14		
								S(B)							~ 2.5	112		
								C							700			
								J1							70			
								J2							69	200		
								Jet E							70 32	322		
								E Total							700	$\frac{261}{1660}$		
								Iotai							700	1000		
	$83 { m Oct} 05$	MV6	0.15	0.15		0.33		C^g							635	648		
								J1							20	59		
								$_{ m E}^{ m J2}$							9 4	44 77		
								r. Total							636	840		
								10141							000	040		

the sensitivity and angular resolution to reveal the features presented in this paper. The core flux density appears to be variable, although observations of similar and high resolution are required to establish the flux density curve reliably. For example, although our value of the core flux density is very similar to the integrated value quoted by Miley & Hartsuijker (1978), their WSRT observations with an angular resolution of 6×6 cosec δ arcsec² includes the flux density from the most prominent knots in the jet as well as the more extended emission (see, also, Barthel et al. 1984). VLBI observations made in 1986 June by Hooimeyer et al. (1992) suggest that the nucleus has a core-jet structure with a dominant nuclear component of flux density 360 mJy and weak emission towards the north-west. From observations at a later epoch, Hooimeyer et al. (1992) also suggest that the core could be superluminal.

2. OBSERVATIONS

Observations were made using the A configuration of the Very Large Array (VLA) of the National Radio Astronomy Observatory¹ at 1465 and 4885 MHz and with the MERLIN telescope at 1666 and 4995 MHz. The source was observed with the VLA for about 10 min at each frequency and calibrated using 3C286 as the primary flux

density and polarization calibrator. The MERLIN observations at 1666 and 4995 MHz were for about 12 and 14 h, respectively. The primary calibrator at 1666 MHz was BL Lac with a flux density of 2.052 Jy while at 4995 MHz the calibrator was 3C84 with a flux density of 59 Jy. The observational parameters and observed properties of the source are summarized in Table 1.

The VLA image at 1465 MHz (Fig. 1), made with an angular resolution of 1.33×1.29 arcsec² along a position angle (PA) of 24°, shows a highly noncollinear structure with two warm-spots towards the south, S(A) and S(B), a prominent nuclear or core component connected to the eastern hot-spot, E, by a curved jet. These features are labeled in Fig. 2. The jet emerges originally towards the north-east, bends abruptly towards the south-east, and then bends gradually back towards the north, feeding the E hot-spot. In addition, there are regions of diffuse extended emission towards the north and northwest of the prominent features. The largest angular size (LAS) of the source defined as the separation of the E hot-spot from S(A) is about 19.6 arcsec which corresponds to a linear extent of 131 kpc in an Einstein-de Sitter universe with $H_0 = 50$ km s⁻¹ Mpc⁻¹. A higher resolution image of the source with a beam size of 0.40×0.40 arcsec² at L band, made by combining the MERLIN and VLA data (Fig. 2), shows greater structural detail of the hot-spots and the jet with two prominent knots of emission, J1 and J2, close to the core. The knot in the jet which is about 7" east of the nucleus is unpolarized (Fig. 1). The higher resolution

¹The National Radio Astronomy Observatory (NRAO) is operated by Associated Universities, Inc. under cooperative agreement with the National Science Foundation.

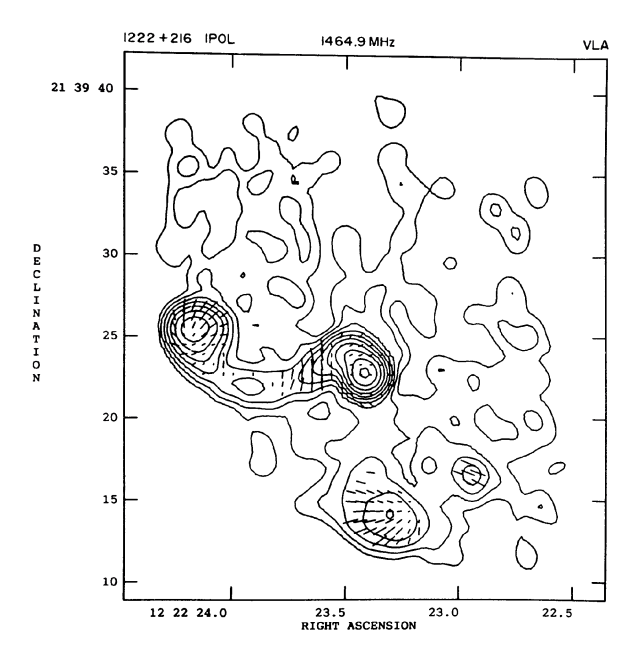


FIG. 1. The VLA image of 1222+216 at 1465 MHz. The resolution is $1"33\times1"29$ along 24°. Percentage polarization is illustrated by the bars along the direction of the E vector, with a vector 1" long corresponding to 33.3%. Contour levels correspond to $(-1, 1, 2, 4, 8, 16, 32, 64, 128, 256, 512)\times1.2$ mJy/beam, and the peak brightness is 704 mJy/beam.

MERLIN+VLA image (Fig. 2) shows this feature to have three components, K1, K2, and K3, the central one of which is nearly transverse to the axis of the jet, reminiscent of knot A in the jet in M87 (Owen et al. 1989). The low observed polarization in the lower resolution image may be due to a change in the orientation of the magnetic field lines possibly due to shocks in the flow of the jet material.

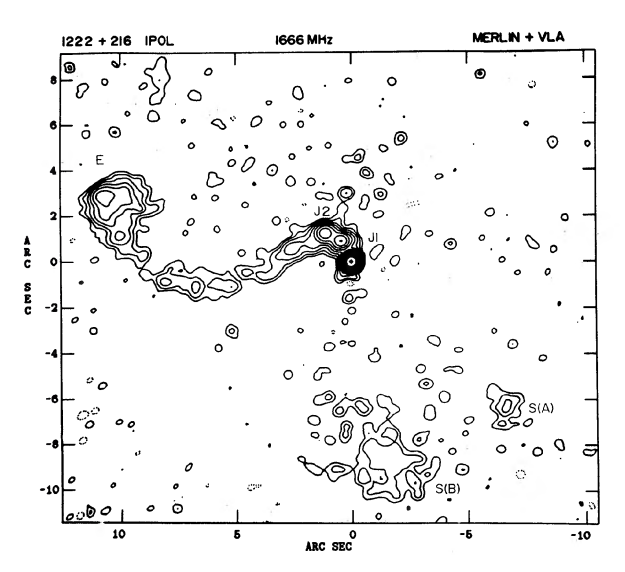


FIG. 2. The combined MERLIN+VLA image of the entire source at $\lambda 18$ cm with an angular resolution of 0".4×0".4. The peak brightness is 700 mJy/beam and the contour levels are (-1, 1, 2, 4, 8, 16, 32, 64, 128, 256, 512, 1024)×0.6 mJy/beam.

We have estimated the spectral indices of some of the features by comparing the MERLIN+VLA image at 18 cm (Fig. 2) with the VLA 6 cm image (Fig. 3) which has a similar angular resolution. The E hot-spot has a spectral index, α ($S \propto v^{-\alpha}$) of about 0.8, while the knots J1 and J2 yield spectral indices of 0.5 and 0.7, respectively using their peak flux densities. The spectral index of the entire jet is about 0.6. Further details of the structure of the knots can be seen in the λ 6 cm image (Fig. 4) which has been made by combining MERLIN and VLA data and has an angular resolution of 0.15×0.15 arcsec². At the location of the abrupt bend in the NE jet there is a suggestion of a sharp edge on the northern side of the second knot, J2; these features could be due to a shock in the flow of the jet caused by a collision with another galaxy or massive gas cloud

In Figs. 1 and 3 the E vectors are superimposed on the total-intensity contours. The source has an integrated rotation measure of -7 ± 2 rad m⁻² with an intrinsic position angle of $123\pm3^{\circ}$ (Simard-Normandin *et al.* 1981). For such a small value of RM, the change from the intrinsic value is only about 17° at $\lambda20$ cm and $\sim1.5^{\circ}$ at $\lambda6$ cm. This suggests that the magnetic field is predominantly aligned along the jet, becoming circumferential in the hotspots as has been seen in many other sources (Bridle & Perley 1984; Saikia & Salter 1988).

3. INTERPRETATION

The low-surface-brightness emissions extending to the NNW (Fig. 1) can probably be attributed to synchrotron emission from old electron populations ejected from the galaxy and the terminal regions of the jets at earlier times. While it is conceivable that the diffuse extended emission which appears clearly only in our lowest resolution image may be generic diffuse emission from the cluster (e.g., Gavazzi & Trinchieri 1983) or some background emission, we consider this highly unlikely. The morphology is strongly suggestive of a connection to the main radio source. These emissions extend roughly 70 kpc from the galaxy and the jet terminal regions. If we ignore the likely expansion of this radio emitting plasma, and assume it was just left behind by the galaxy and associated jets as they moved towards the SSE, then the projected galaxy speed is, $v_g \approx 700 \text{ km s}^{-1} t_8^{-1}$, where t_8 is the time in units of 10^8 yr that this source has been emitting radio plasma. There is not enough multifrequency data available to allow us to estimate the age of this source from spectral aging calculations (e.g., Alexander & Leahy 1987; Leahy et al. 1989; Siah & Wiita 1990), but this technique typically yields lifetimes of 0.03-0.7 t₈; arguments based on source statistics and jet propagation distances (e.g., Schmidt 1988; Rosen 1989; Wiita & Gopal-Krishna 1990) tend to give values of $t_8 > 1$.

The suggested motion of the galaxy could also consistently explain both the final bending of the jet towards the north near the hotspot, E, and the curvature of the flow in the southern lobe from S(B) to S(A) after they emerge from the galaxy's protective interstellar medium (ISM).

1661 SAIKIA *ET AL*.: 1222+216 1661

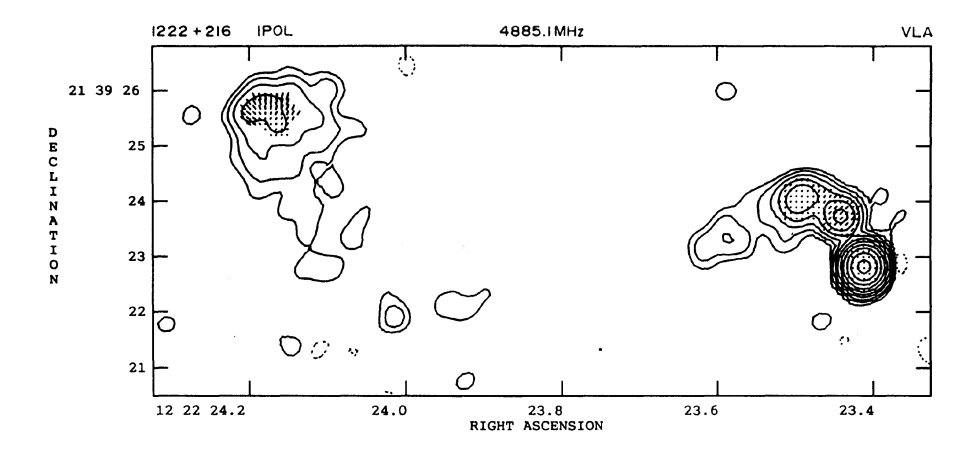


FIG. 3. VLA map of the core and eastern features at 4885 MHz; the resolution is 0.42×0.40 along -0.8. Here a polarization bar of 0.1" corresponds to 33.3%. Contour levels are at -1, 1, 2, 4, 8, 16, 32, 64, 128, 256, 512 mJy/beam, and the peak brightness is 650 mJy/beam.

Although this flow pattern from S(B) to S(A) is suggested by the brightness distribution shown in Fig. 1, it is not inconceivable that the flow may be from S(A) to S(B). A more sensitive high-resolution image to trace the counterjet is required to confirm our assumption. While the width of the jet, r_j , is not very well defined from these observations, and the bending scale length or radius of curvature, R, is also uncertain, reasonable estimates are: $r_j \approx 2$ kpc and $R \approx 40$ kpc, respectively.

Reasonable values for the galactic velocity, v_g would be in the range of $100-800 \text{ km s}^{-1}$; the upper end of this range is plausible even for the brightest and possibly most massive galaxy in a cluster (see Gebhardt & Beers 1991), which is expected to be hosting the active galactic nucleus. As is well known, there are only very weak a priori limits on the speed of the flow down the jet, with lower bounds for v_j of a few thousand km s⁻¹ and the upper bound being nearly c. Assuming that the jet flow is nonrelativistic but substantially supersonic and the equation of state is dominated by thermal particles, then one has the simple relation (e.g., Jones & Owen 1979; O'Dea 1985)

$$\frac{n_j v_j^2}{R} \approx \frac{n_{\rm ICM} v_g^2}{r_i},$$

where v_i is the flow speed down the jet and n_i and n_{ICM} are the densities of the jet fluid and intracluster medium, respectively. A fairly wide range of parameters are consistent with the data at hand, but a reasonable set, typical of many bent sources (e.g., O'Dea 1985) would be: $n_{ICM} = 5 \times 10^{-4} \text{ cm}^{-3}$, $n_j = 10^{-6} \text{ cm}^{-3}$, $v_g = 500 \text{ km s}^{-1}$, and v_j =50 000 km s⁻¹. The lack of any x-ray map means that there are essentially no constraints on the density and temperature of the ICM. This ignorance, coupled with uncertainties in R and r_j , leads to a wide range of possible jet velocities v_i . For example, if we still take R=40 kpc and $v_g = 500 \text{ km s}^{-1}$, but assume $n_{ICM} = 8 \times 10^{-4} \text{ cm}^{-3}$, $n_i = 4$ $\times 10^{-7}$ cm⁻³, and $r_j = 1$ kpc, then $v_j = 1.4 \times 10^5$ km s⁻¹, or nearly c/2; this high value is compatible with those suggested from the flux ratio arguments given in the next paragraph. Even higher jet velocities could be consistent with the observations and a dynamical pressure bending of a very light jet. On the other hand, low values, such as

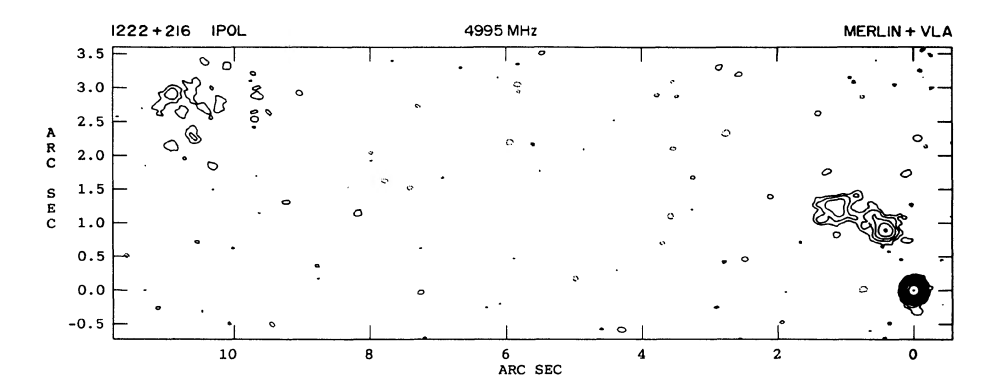


FIG. 4. The MERLIN+VLA map of the eastern features at $\lambda 6$ cm with a resolution of 0".15×0".15. Contour levels correspond to $(-1, 1, 2, 4, 8, 16, 32, 64, 128, 256, 512) \times 1.2$ mJy/beam, and the peak brightness is 636 mJy/beam.

1662 SAIKIA *ET AL*.: 1222+216 1662

 $v_j \approx 6000 \text{ km s}^{-1}$ are possible if $n_{\text{ICM}} = 3 \times 10^{-4} \text{ cm}^{-3}$, $n_j = 10^{-5} \text{ cm}^{-3}$, $r_i = 2 \text{ kpc}$, R = 40 kpc, and $v_g = 250 \text{ km s}^{-1}$.

The one-sided jet feeds the eastern lobe, which has a hot-spot whose peak is about 10 times brighter than the hot-spot on the SW side. The most widely accepted general explanation for brightness asymmetries is Doppler boosting of the approaching emission (e.g., Blandford & Königl 1979), such that the observed flux density S(v) is given by

$$S(v) = S_{em}(v) [\gamma(1-\beta\cos\theta)]^{-(2+\alpha)}$$

where $S_{\rm em}(\nu)$ is the emitted flux density, θ is the angle between the jet and the line of sight, $\beta = v_j/c$ and $\gamma = (1 - \beta^2)^{-1/2}$. If the jets are intrinsically nearly oppositely directed and have identical v_i 's, then

$$\beta \cos \theta = \frac{(S_{\rm E}/S_{\rm S})^{1/(2+\alpha)} - 1}{(S_{\rm E}/S_{\rm S})^{1/(2+\alpha)} + 1} = \frac{y - 1}{y + 1} \approx 0.55,$$

where the subscripts E and S refer to the eastern and southern jets, and $y \approx 3.4$ is estimated from the peaks of emission in the jets when we use $\alpha = 0.6$. So $v_i \approx c/2$ can suffice for the approaching jet nearly along the line of sight, but for θ =45°, $\beta \approx 0.78$ suffices to explain the entire asymmetry. This is an upper limit since the brightness asymmetry is dominated by the knots J1 and J2 which we suggest are due to an interaction of the jet with a dense cloud or galaxy. Hence there is consistency between these estimates for v_i and the range obtained in the previous paragraph. For the rest of the jet and the hot-spots the velocities required are only mildly relativistic. The velocity estimates are similar to those required to explain the brightness asymmetry of the jets in well-observed quasars of comparable luminosity, as well as for the limits in the brightness ratio of the hot-spots in most one-sided radio sources (Saikia et al. 1984). We can thus conclude that hypersonic jets, with $\beta > 0.6$ can both be bent for reasonable ICM and jet parameters and can supply enough Doppler boosting to explain most, if not all, of the jet/counter-jet brightness asymmetry. We note that within the unified scheme of, e.g., Barthel (1989), QSRs should all have $\theta \le 45^\circ$, so the above constraints on the viewing angle are not unreasonable. Finally, this source has a relatively large fraction of its flux density emerging from the core ($\sim 70\%$ at 5 GHz), which is also consistent with some Doppler beaming enhancements in any unified scheme.

The pair of knots J1 and J2, possibly indicating shocks (e.g., Norman et al. 1982), and the suggestion of a sharp edge in J2 are consistent with this abrupt deflection being induced by a collision between the jet and gas associated with a nearby small companion galaxy, conceivably one in the process of being cannibalized by the host of the QSR, or by a dense cloud in the parent galaxy itself. The abruptness of this bend is in clear contrast to the much gentler bending farther out along the jet, and argues for the collision hypothesis. While no such galaxy has been seen in Hintzen's CCD frame of the 1222+216 region (H84), it would be difficult to detect such an object because of its low brightness and close proximity to the quasar nucleus.

The possibility of a radio plasmoid being deflected by an external gas cloud was proposed by Christiansen et al. (1984). There are several good observational candidates for radio jets from quasars interacting with external clouds or galaxies (HUO; Christiansen et al. 1984). The best of these is 3C 275.1, where a galaxy is seen at the location of the bend and the observed bending can be nicely explained in terms of a collision of a jet with that galaxy's halo (Stocke et al. 1985). The case for collisional bending is made stronger for this source because the galaxy shows strong [O II] emission, suggesting that the impact of the radio jet excited the companion galaxy's ISM (Hintzen & Romanishin 1986). Furthermore, the significant depolarization of the radio emission from 3C 275.1 in the vicinity of that galaxy (Liu & Pooley 1990) also argues for its playing the role of the deflector. In a different source, the quasar 3C 48 appears to have a jet which was completely disrupted by an interaction with a dense cloud within the body of the host galaxy itself (Wilkinson et al. 1991).

Serious doubts about whether a jet's direction could be significantly affected by a collision that would still leave the jet stable were strengthened by the numerical simulations of De Young (1991) who concluded such a "refraction" was unlikely to occur. However, recent three-dimensional (3D) hydrodynamical simulations using a more sophisticated code with less numerical viscosity have shown that jets could indeed be stably bent under these conditions; typically, two internal shocks could accomplish this refraction, with essentially a deLaval nozzle forming in the jet/ cloud interaction region (Balsara & Norman 1993). As noted above, the observed knots could arise from such shocks. A different 3D hydrodynamics code, including dynamically unimportant magnetic fields, also led to an apparently stable bending of a jet by about 90° via a collision with a dense cloud (Clarke 1992), although some radio emitting material flows to the other side of the cloud.

Oscillatory instabilities may be present (e.g, Hardee 1984), and might provide an alternative explanation for the bends in the jet. Assuming hydrodynamical (essentially Kelvin-Helmholtz) instabilities for an adiabatically expanding jet, Hardee (1984) shows that the fastest growing mode has a wavelength,

$$\lambda_{\text{max}} \approx \left(\frac{4.2M_{\text{in}}}{1+\eta^{1/2}}-2.5\right)r$$

where $M_{\rm in} = v_j/a_j$, with a_j the sound speed in the jet, r the radius of the jet and $\eta = n_j/n_{\rm ICM}$. Following our earlier discussion, where all reasonable values for n_j were seen to be much less than those for $n_{\rm ICM}$, we assume $\eta \ll 1$. If the observed bend in the inner part of the jet is caused by such an instability, and the observed oscillation distance is identified with $\lambda_{\rm max} \approx 35$ kpc, then for $r \approx 1$ kpc we must have $M_{\rm in} \approx 9$. While there may be small oscillations further out in the jet, they are not clearly detected in our maps. If we identify the large scale bending towards the end of the E jet with a maximally growing wavelength, then $\lambda_{\rm max} \approx 80$ kpc, yielding $M_{\rm in} \approx 20$. From a more recent analysis on the spatial stability of jets, which examines the relative importance

of the fundamental and reflection solutions, Hardee (1987) suggests

$$\lambda_{\text{max}} \approx 5.2 M_{\text{in}} r / (0.66 + \eta^{1/2}).$$

Using this expression, the corresponding values of $M_{\rm in}$ for the bends near the core and the E hot-spot are ≈ 4 and 10, respectively. In the intermediate portion of the jet, there are suggestions of low-amplitude oscillations, although for hydrodynamical instabilities one expects the amplitudes of the oscillations to grow with distance down the jet (Hardee 1984). While the values of the Mach number seem reasonable, we need to make observations to better determine the ridge line of the jet in order to examine this scenario more critically.

Precession can yield a wide range of projected morphologies, especially in sources inclined at small angles to the line of sight (e.g., Gower et al. 1982; Zaninetti 1989). The moderately prominent core, its variability, and possible superluminal motion are all consistent with a small angle of inclination to the line of sight. However, the polarization distribution and the orientation of the magnetic field in the region where the jet bends sharply near the core and also in S(B) (see Fig. 1) are suggestive of field lines which have been sheared to lie along the flow directions. Such a shearing may be due to interaction with a clumpy external environment, but would not naturally arise in a precession model.

We must also mention the possibility that magnetic fields play an important role in the dynamics of this source. In their study of the archetypal low-luminosity radio galaxy 3C465, Eilek et al. (1984) suggested that magnetic fields in the ICM of $\sim 10^{-7}$ G could be adequate to bend a current-carrying jet and produce a C-shaped structure with a cluster field which is toroidal and in the plane of the jet. There is very little evidence for or against this hypothesis in our case, but the abrupt inner bend and the reversing outer bends would certainly require specialized field configurations.

While we feel the arguments for a combination of collisional and ram-pressure bending in the case of 1222+216 are good, they are certainly not conclusive. Deeper imaging to search for the putative interacting galaxy (as is seen in 3C 275.1; Stocke *et al.* 1985) is needed, as is a careful x-ray measurement to search for extensive hot gas around the host galaxy (as is again present for 3C 275.1; Hintzen & Romanishin 1986).

4. RADIO STRUCTURES AND CLUSTER MEMBERSHIP

H84 suggested that the more distorted, noncollinear quasars tend to occur in richer galaxy environments than the collinear sources. As has been recently shown by Ellingson et al. (1991) only 3 of 63 quasars in their sample (chosen to have m > 17.5 and 0.3 < z < 0.6) have quasargalaxy spatial covariance amplitudes, $B_{gq} > 1000$, which are high enough to qualify as members of rich clusters. Two of these three quasars in very dense environments are 3C 275.1 and 3C 215, the best instances of "radio-tail quasars" in H84. It has also been known for some time that

TABLE 2. The sample of quasars.

Source	Alt. name	Redshift	$\Delta N_{lim}/A$	P _{5GHz} (ext.) W Hz ⁻¹ sr ⁻¹	LAS	l kpc	Δ	f_c	Ref.
(1)	(0)	(0)	(4)		(0)		(0)	(9)	(10)
(1)	(2)	(3)	(4)	(5)	(6)	(7)	(8)	(9)	(10)
0003 + 158	4C15.01	0.450	+10	25.30	31.5	214	3	0.37	1
0115 + 027	3C37	0.672	-5	25.94	13.3	105	1	0.23	2,3
0118 + 034	3C39	0.765	+5	25.89	47.0	383	9	0.07	1,2,4
0130 + 242	4C24.02	0.457	+10	25.26	53.4	366	9	0.32	1,5,6
0214+108	4C10.06	0.408	+10	25.40	119.0	773	10	0.21	1
				05.00	00.0	100		0.01	* 0
0340+048	3C93	0.357	0	25.66	26.9	163	11		7,8
0903 + 169	3C215	0.411	+30	25.42	43.0	280	50	0.07	2,4,9
0957+003	4C00.34	0.907	0	26.03	33.5	282	21	0.19	2,4
1038+52A	OL564	0.677	0	25.11	36.8	291	28	0.86	10
1100+772	3C249.1	0.311	+10	25.40	39.0	219	9	0.16	4,9,11
1218+339	3C270.1	1.519	0	26.94	9.3	79	36	0.16	12
1222+216	4C21.35	0.435	+40	25.42	19.6	131	68	0.70	This paper
1241+166	3C275.1	0.557	+70	26.01	17.7	131	22	0.16	12
1335-061	4C-06.35	0.625	+25	20.01				0.10	
1423+242	4C24.31	0.649	+10	25.87	20.2	158	25	0.29	2,5
1512+370	4C37.43	0.371	+40	25.26	50.9	315	1	0.11	5
1618+177	3C334	0.555	+20	25.76	46.0	341	3	0.21	2,4,6
1741+279	4C27.48	0.372	+30	24.93	9.2	57	26	0.58	2,3
2353+283	4C28.59	0.731	+05	25.67	9.7	78	28	0.27	2,5

Reference

Miley & Hartsuijker (1978);
 Hintzen, Ulvestad & Owen (1983);
 Saikia et al. (1984);
 Potash & Wardle (1979);
 Wardle & Potash (1982);
 Wills (1979);
 Hutchings, Price & Gower (1988);
 Pooley & Henbest (1974);
 Owen, Wills & Wills (1980);
 Lonsdale & Morison (1983);
 Stocke, Burns & Christiansen (1985).

there is a reasonably strong correlation between the degree of misalignment, Δ , the supplement of the angle formed at the nucleus by the outer hot-spots, and f_{ϕ} the fraction of emission from the radio core (e.g., Saikia et al. 1991 and references therein). In the relativistic beaming models, f_c is used as a statistical indicator of orientation of the source axis to the line of sight, and the large values of Δ are then ascribed to amplification of small misalignments due to projection effects in sources inclined at small angles to the line of sight. It is of interest to determine which of these two is the primary effect responsible for the large observed distortions in the structure of quasars. While a more extensive study is in progress, we attempt to investigate this aspect here using the sample of quasars observed by H84. In Table 2 we summarize some of the properties for this sample of quasars. Columns (1) and (2) give the coordi-

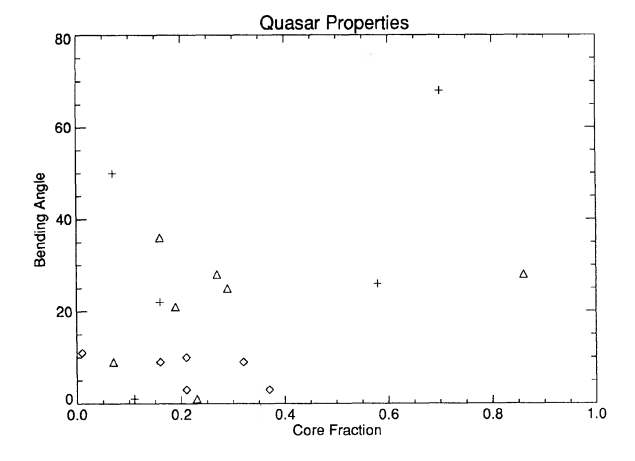


FIG. 5. Bending angle (Δ) plotted against fraction of total radio flux density in the core (f_c) for the sample of quasars listed in Table 2. Quasars with $z \leqslant 0.6$ and $\Delta N_{\text{lim}}/A > 30$ are denoted by $\dot{+}$, those with $z \leqslant 0.6$ and $\Delta N_{\text{lim}}/A < 30$ are denoted by \Diamond , while those with z > 0.6 and $\Delta N_{\text{lim}}/A < 30$ are denoted by Δ . $\Delta N_{\text{lim}}/A$ is a measure of the number of excess galaxies in the vicinity of the quasar, as defined by Hintzen (1984).

nates and alternative name, column (3) the redshift, and column (4) a measure of cluster richness from H84 which is a measure of excess number density of galaxies, $\Delta N_{\rm lim}/A$, in the vicinity of the quasar. The extended radio power at 5 GHz is given in column (5), the largest angular size and the corresponding linear size in columns (6) and (7), the misalignment or bending angle, Δ in column (8), and the fraction of radio flux density in the core at an emitted frequency of 8 GHz, f_c , in column (9). References for the radio data are given in the final column. The source 1335 -061 (4C-06.35) from H84 has been excluded from the discussion since from the presently available image (HUO), the identification of the nuclear component, and also the bending angle, is uncertain.

In Fig. 5 we plot Δ against f_c for the quasars in Table 2. Concentrating only on those sources at relatively low redshifts, z < 0.6, where cluster identification is reasonably complete (H84), all sources which are significantly distorted, ($\Delta \ge 15^\circ$), are found in relatively rich clusters $(\Delta N_{\text{lim}}/A \geqslant 30)$. Only one of the five low z, dense environment sources has a small bending angle. Conversely, all six of the low redshift sources in relatively low density environments exhibit only small deviations from collinearity (see H84). To assess the importance of projection effects in the framework of the relativistic beaming scenario, let us consider the sources which are highly core-dominated, $f_c \ge 0.5$, namely 1038+52A, 1222+216, and 1741+279. Of these, 1038 + 52 A is not in the low-redshift subsample, while 1222+216 and 1741+279 are highly distorted and also occur in rich galaxy environments. While one requires a larger sample to address the question satisfactorily, the following scenario seems plausible. In relatively weak cored sources in rich environments, such as 3C215 and 3C275.1 the observed distortions are largely due to interactions with the environment, while in the case of the coredominated sources it is possibly due to a combination of both environmental and projection effects, with the latter often playing a dominant role. Although the mounting evidence in favor of relativistic beaming justifies our assumption of using the relative core strength as a statistical indicator of orientation, it would be of interest to determine any possible role of the environment on the observed strength of the radio core. We also attempted to determine any difference in the extended radio luminosity either between the sources in richer and poorer environments or between the collinear and distorted quasars, but did not find any evidence of it. There does not appear to be a high-luminosity analogue of the Fanaroff-Riley classification scheme.

This paper is dedicated to the memory of Joan Adams who took great care and pains to see through the publication of many of our papers. We thank Susan Neff for useful discussions, Peter Thomasson for assistance with the MERLIN observations and Tim Cornwell and Chris Salter for their efforts in helping with the VLA observations. We thank the referee for many useful suggestions and comments which helped to improve the presentation and discussion in the paper. This work is supported in part by NSF Grant No. AST9102106 and by Smithsonian Institution Grant No. FR10263600.

REFERENCES

Alexander, P., & Leahy, J. P. 1987, MNRAS, 225,1 Balsara, D., & Norman, M. L. 1993, ApJ (in press) Barthel, P. D. 1989, ApJ, 336, 606 Barthel, P. D., Miley, G. K., Schilizzi, R. T., & Preuss, E. 1984, A&A, Begelman, M. C., Rees, M. J., & Blandford, R. D. 1979, Nature, 279, 770 A&A, 261, 25 Blandford, R. D., & Königl, A. 1979, ApJ, 232, 34 Bridle, A. H., & Perley, R. A. 1984, ARA&A, 22, 319 Christiansen, W. A., Burns, J. O., & Stocke, J. T. 1984, in Physics of Energy Transport in Extragalactic Radio Sources, edited by A. H. Bridle and J. A. Eilek (NRAO, Green Bank), p. 83 Clarke, D. A. 1992, in Proceedings of the Ringberg Workshop on Jets in Extragalactic Radio Sources, edited by H.-J. Röser and K. Miesenheimer (Springer, Berlin) (in press) De Young, D. S. 1991, ApJ, 371, 69 Eilek, J. A., Burns, J. O., O'Dea, C. P., & Owen, F. N. 1984, ApJ, 278, A&A, 113, 285 Ellingson, E., Yee, H. K. C., & Green, R. F. 1991, ApJ, 371, 49 Fanti, C., Fanti, R., Schilizzi, R. T., Spencer, R. E., & van Breugel, W. J. M. 1986, A&A, 170, 10 Gavazzi, G., & Trinchieri, G. 1983, ApJ, 270, 410 Gebhardt, K., & Beers, T. C. 1991, ApJ, 383, 72 Gower, A. C., Gregory, P. C., Hutchings, J. B., & Unruh, W. G. 1982, ApJ, 262, 478

Hardee, P. E. 1984, ApJ, 287, 523

Hardee, P. E. 1987, ApJ, 313, 607

A. G. 1983, ApJ, 270, 39 Hintzen, P. 1984, ApJS, 55, 533 (H84)

Harris, D. E., Dewdney, P. E., Costain, C. H., Butcher, H., & Willis,

Hintzen, P., Boeshaar, G. O., & Scott, J. S. 1981, ApJ, 246, L1 Hintzen, P., & Romanishin, W. 1986, ApJ, 311, L1 Hintzen, P., & Stocke, J. 1986, ApJ, 308, 540 Hintzen, P., Ulvestad, J., & Owen, F. 1983, AJ, 88, 709 (HUO) Hooimeyer, J. R. A., Schilizzi, R. T., Miley, G. K., & Barthel, P. D. 1992, Hutchings, J. B., Price, R., & Gower, A. C. 1988, ApJ, 329, 122 Jones, T. W., & Owen, F. N. 1979, ApJ, 234, 818 Leahy, J. P., Muxlow, T. W. B., & Stephens, P. W. 1989, MNRAS, 239, Liu, R., & Pooley, G. 1990, MNRAS, 245, 17P Lonsdale, C. J., & Morrison, I. 1983, MNRAS, 203, 833 Miley, G. K., & Hartsuijker, A. P. 1978, A&AS, 34, 129 Neff, S. G. 1982, Ph.D. thesis, University of Virginia Norman, M. L., Smarr, L., Winkler, K.-H. A., & Smith, M. D. 1982, O'Dea, C. P. 1985, ApJ, 295, 80 O'Donoghue, A. A., Owen, F. N., & Eilek, J. A. 1990, ApJS, 72, 75 Owen, F. N., Hardee, P. E., & Cornwell, T. J. 1989, ApJ, 340, 698 Owen, F. N., Wills, B. J., & Wills, D. 1980, ApJ, 235, L57 Pearson, T. J., & Readhead, A. C. S. 1988, ApJ, 328, 114 Pooley, G. G., & Henbest, S. N. 1974, MNRAS, 169, 477 Potash, R. I., & Wardle, J. F. C. 1979, AJ, 84, 707 Riley, J. M., & Pooley, G. G. 1978, MNRAS, 184, 769 Rosen, A. 1989, Ph.D. thesis, Georgia State University Saikia, D. J., & Salter, C. J. 1988, ARA&A, 26, 93 Saikia, D. J., Shastri, P., Sinha, R. P., Kapahi, V. K., & Swarup, G. 1984, Saikia, D. J., Singal, A. K., & Wiita, P. J. 1991, in Variability of Active

Galactic Nuclei, edited by H. R. Miller and P. J. Wiita (Cambridge University Press, Cambridge), p. 160

Saikia, D. J., Staveley-Smith, L., Wills, D., Cornwell, T. J., Salter, C. J., Junor, W., & Shastri, P. 1987, MNRAS, 229, 495

Schmidt, M. 1988, in Active Galactic Nuclei, edited by H. R. Miller and P. J. Wiita (Springer, Berlin), p. 408

Siah, M. J., & Wiita, P. J. 1990, ApJ, 363, 411

Simard-Normandin, M., Kronberg, P. P., & Button, S. 1981, ApJS, 45, 97 Smith, E. P., & Heckman, T. M. 1990, ApJ, 348, 38

Stocke, J., Burns, J. O., & Christiansen, W. A. 1985, ApJ, 299, 799

Swarup, G., Sinha, R. P., & Hilldrup, K. 1984, MNRAS, 208, 813

Wardle, J. F. C., & Potash, R. I. 1982, in Extragalactic Radio Sources, IAU Symposium No. 97, edited by D. S. Heeschen and C. M. Wade (Reidel, Dordrecht), p. 129

Wiita, P. J., & Gopal-Krishna 1990, ApJ, 353, 476

Wilkinson, P. N., Tzioumis, A. K., Benson, J. M., Walker, R. C., Simon, R. S., & Kahn, F. D. 1991, Nature, 352, 313

Wills, D. 1979, ApJS, 39, 291

Yee, H. K. C., & Green, R. F. 1984, ApJ, 280, 79

Yee, H. K. C., & Green, R. F. 1987, ApJ, 319, 28

Zaninetti, L. 1989, A&A, 221, 204